New Phytologist

Research

Abscisic acid-controlled redox proteome of *Arabidopsis* and its regulation by heterotrimeric Gβ protein

Amanda L. Smythers[1], Nikita Bhatnagar[2], Chien Ha[2], Parinita Majumdar[2], Evan W. McConnell[1], Boominathan Mohanasundaram[2], Leslie M. Hicks[1] and Sona Pandey[2]

[1]The University of North Carolina at Chapel Hill, Chapel Hill, NC 27599, USA; [2]Donald Danforth Plant Science Center, St Louis, MO 63132, USA

Author for correspondence:
Sona Pandey
Email: spandey@danforthcenter.org

Received: *1 April 2022*
Accepted: *18 June 2022*

New Phytologist (2022) **236:** 447–463
doi: 10.1111/nph.18348

Key words: abscisic acid, AGB1, Arabidopsis, G-protein, photosynthesis, proteomics, redox, redox proteomics.

Summary

- The plant hormone abscisic acid (ABA) plays crucial roles in regulation of stress responses and growth modulation. Heterotrimeric G-proteins are key mediators of ABA responses. Both ABA and G-proteins have also been implicated in intracellular redox regulation; however, the extent to which reversible protein oxidation manipulates ABA and/or G-protein signaling remains uncharacterized.
- To probe the role of reversible protein oxidation in plant stress response and its dependence on G-proteins, we determined the ABA-dependent reversible redoxome of wild-type and Gβ-protein null mutant *agb1* of Arabidopsis.
- We quantified 6891 uniquely oxidized cysteine-containing peptides, 923 of which show significant changes in oxidation following ABA treatment. The majority of these changes required the presence of G-proteins. Divergent pathways including primary metabolism, reactive oxygen species response, translation and photosynthesis exhibited both ABA- and G-protein-dependent redox changes, many of which occurred on proteins not previously linked to them.
- We report the most comprehensive ABA-dependent plant redoxome and uncover a complex network of reversible oxidations that allow ABA and G-proteins to rapidly adjust cellular signaling to adapt to changing environments. Physiological validation of a subset of these observations suggests that functional G-proteins are required to maintain intracellular redox homeostasis and fully execute plant stress responses.

Introduction

Plants are sessile organisms with fascinating adaptive mechanisms to optimize growth and development under unfavorable conditions. Phytohormones such as abscisic acid (ABA), brassinosteroids, cytokinins and strigolactones act cooperatively to modulate adaptive responses (Ha *et al.*, 2014; Kuromori *et al.*, 2018). Abscisic acid not only serves as a signal for several abiotic stresses, but also enables plants to balance their energy allocation for growth and development with that needed to alleviate stress by regulating photosynthesis under abiotic stress conditions (Foyer, 2018). In aboveground parts, ABA acts primarily through the stomatal aperture; plants promote stomatal closure in response to both drought and ABA treatment to help retain water. Smaller stomatal apertures result in decreased transpiration as well as the inhibition of photosynthesis, thereby modulating the established energy balance (Gururani *et al.*, 2015; Albert *et al.*, 2017; Kuromori *et al.*, 2018).

Decreased transpiration and photosynthesis result in the accumulation of reactive oxygen/nitrogen species (ROS/RNS) followed by an alteration of redox homeostasis (Zhou *et al.*, 2013; Song *et al.*, 2014; Qi *et al.*, 2018). Once hypothesized to be markers of stress, ROS/RNS are now known to play an essential role in modulating signaling and metabolic pathways in response to stress (Apel & Hirt, 2004; Mittler, 2017; Fichman *et al.*, 2019; Huang *et al.*, 2019). Precise spatial and temporal regulation of ROS/RNS generation and dissipation is required for maintaining normal plant physiology and function (Suzuki *et al.*, 2013; Postiglione & Muday, 2020). Protein cysteine thiols are particularly susceptible to oxidation by ROS and RNS and are capable of forming an array of physiologically significant post-translational modifications, including disulfide bonds, sulfenylation, *S*-nitrosylation, *S*-glutathionylation and persulfidation, among others (Ying *et al.*, 2007; Fra *et al.*, 2017). Further, reversible oxidative signaling is propagated through redox enzymes such as thioredoxin and glutaredoxin to regulate cellular metabolic activities (López-Grueso *et al.*, 2019).

Abscisic acid is a known modulator of redox changes in plants and therefore must employ reversible oxidative signaling for rapid proliferation of intracellular signals following environmental stimuli (Hossain & Dietz, 2016; Noctor *et al.*, 2018; Chapman *et al.*, 2019). Abscisic acid has a substantial effect on differential expression of proteins related to photosynthesis (a key contributor to intracellular ROS accumulation), redox homeostasis and

stress signaling (Alvarez *et al.*, 2011, 2013). Additionally, ABA-triggered persulfidation has been connected to regulation of stomatal guard cell function and autophagy in Arabidopsis, demonstrating cysteine thiols as an essential component of ABA signaling pathways (Chen *et al.*, 2020; Laureano-Marín *et al.*, 2020; Shen *et al.*, 2020). However, there is only a nascent understanding of proteins modulated in the redox state by ABA.

Heterotrimeric G-proteins are universal signaling proteins in eukaryotes and are established mediators of ABA signaling and redox regulation in plants (Pandey *et al.*, 2009; Alvarez *et al.*, 2013; Torres *et al.*, 2013; Xu *et al.*, 2015). The G-protein heterotrimer consists of one Gα protein subunit, one Gβ protein subunit and one Gγ protein subunit, which alternate between signal-dependent inactive, associated (GDP-Gαβγ) and active, dissociated (GTP-Gα and Gβγ) forms (Pandey, 2019). In *Arabidopsis thaliana*, the G-protein complex is represented by four Gα (one canonical Gα, GPA1, and three extra-large Gα, XLGα1–3), one Gβ (AGB1) and three Gγ (AGG1–3) proteins (Pandey, 2019). Specific Gα and Gγ proteins interact with the single Gβ protein to form distinctive heterotrimeric complexes. This unique G-protein repertoire in Arabidopsis allows the absence of the sole functional AGB1 (*agb1* mutant) to effectively represent the loss of all heterotrimeric G-protein function (Urano *et al.*, 2016; Roy Choudhury *et al.*, 2020). AGB1 is critical for multiple biological processes including growth, architecture, immune response, stomatal development/movement, salinity and drought stress response, supporting the central role of G-proteins in regulating plant form and physiology (Nilson & Assmann, 2010; Chakravorty *et al.*, 2015; Yu & Assmann, 2015; Urano *et al.*, 2016; Liang *et al.*, 2017; Roy Choudhury *et al.*, 2020). Surprisingly, only a few effectors of AGB1 are known. Despite its functional and genetic link with the key ROS-producing NADPH oxidases AtRbohD and AtRbohF in Arabidopsis (Torres *et al.*, 2013), the role of AGB1 in regulating oxidative signaling has not been explored.

To determine the role of reversible protein oxidation in plant stress response and its dependence on G-proteins, the *agb1* null mutant (representing the loss of G-protein function) was compared with wild-type (WT) Col-0 plants in the presence or absence of ABA (as a proxy for abiotic stresses). Comprehensive global and redox proteomics combined with physiological measurements demonstrate that ABA modifies global protein redox status in a G protein-dependent manner, altering multiple signaling and metabolic networks to regulate a multitude of biological processes.

Materials and Methods

Plant growth, stress treatment and measurement of physiological parameters

Arabidopsis thaliana WT (Col-0) and *agb1-2* mutant plants (Ullah *et al.*, 2003) were grown side-by-side on media containing ½ Murashige & Skoog medium (½MS), 1% sucrose, 1% agar, pH 5.7 in a growth chamber (16 h : 8 h, light : dark, 200 μmol s^{-1} m^{-2} light intensity, 22°C) for 14 d. Pooled seedlings from 10 plates were treated with ABA (100 μM) or an equal amount of EtOH (control) for 2 h and frozen in liquid N_2.

For the quantification of physiological parameters, we obtained an additional allele of *agb1* (salk_204268C, stock no. N692967) from the Arabidopsis Biological Resource Center (ABRC), confirmed it by genotyping and named it *agb1-5*. Two independent alleles of the *MAPK14* gene (Lv *et al.*, 2021) were also obtained from ABRC. *agb1-2*, *agb1-5*, *mapk14-1* and *mapk14-2* mutants and WT plants were grown for 5 wk in growth chambers. Various photosynthetic parameters, such as F'_q/F'_m, nonphotochemical quenching (NPQ), electron transfer rate (ETR) and anthocyanin index were quantified by the Phenovation CropReporter system at 0 and 4 h after dehydration treatment. For ROS and starch content measurement, plants were grown on MS media plates for 14 d and treated with 50 μM ABA for 2 h. Seedlings were stained with nitroblue tetrazolium (NBT) to detect superoxide and with 3,3′-diaminobenzidine (DAB) to detect hydrogen peroxide. For quantification of ROS staining, the total number of pixels occupied by the Arabidopsis rosette and the number of brown or blue pixels (produced by NBT and DAB, respectively) within that rosette was measured using the Python libraries OpenCV and NumPy (Gehan *et al.*, 2017; Harris *et al.*, 2020). The percentage of colored pixels is used to represent the ROS content. Lugol's reagent was used to stain for starch and imaged as previously described (Nguyen *et al.*, 2017). WT, *agb1* and *mapk14* mutant seeds from the same batch were used for the inhibition of germination assays. Seeds were sown on plates containing different amounts of ABA and grown in growth chambers. Germination, defined as breakage of the seed coat and emergence of the radicle, was measured at 48 h poststratification.

Protein extraction

All groups had four biological replicates. Liquid N_2 ground samples (*c.* 100 mg each) were mixed with 1 ml of cold 10% trichloroacetic acid (TCA) in acetone, briefly vortexed and incubated at −20°C for 30 min before centrifugation for 5 min at 20 000 ***g*** and 4°C. The supernatant was removed and the pellet was washed with 1 ml cold acetone and resuspended in 0.5 ml lysis buffer (50 mM Tris–HCl pH 8, 100 mM NaCl, 100 mM diethylene triamine pentaacetic acid (DTPA), 0.5% SDS and 4 M urea) containing 100 mM iodoacetamide (IAM) to block reduced thiols, and incubated in the dark for 2 h at room temperature with shaking. Cellular debris was separated from soluble proteins by centrifugation and the supernatant was added to 10 ml of cold acetone and incubated for 30 min at −20°C to precipitate proteins and remove excess IAM. Following centrifugation for 5 min at 3220 ***g*** and 4°C, the pellet was resuspended in 0.5 ml lysis buffer. Protein concentration was estimated using the CB-X Protein Assay (G-Biosciences, St Louis, MO, USA) and adjusted to 1 mg ml^{-1} for normalization.

Enrichment of reversible cysteine oxidation

Protein-level enrichment of reversible cysteine oxidation was performed as described previously (McConnell *et al.*, 2018;

Smythers *et al.*, 2020). To show that alkylation of reduced cysteines was complete and to reduce false positive changes in reversible oxidation, a negative enrichment control was generated by pooling 15 µg from every sample (480 µg total) and then mock-reduced with water. Samples (500 µg) were incubated with 10 mM dithiothreitol (DTT) for 1 h to reduce cysteine residues with any reversible oxidation back to a free thiol. Excess reducing agent was removed by adding samples to 10 ml of cold acetone and incubating at −20°C for 1 h. Following centrifugation, the protein pellet was dissolved in 500 µl resuspension buffer (50 mM Tris–HCl pH 8, 0.5% SDS and 4 M urea).

Thiopropyl Sepharose 6B resin (GE Healthcare, Boston, MA, USA) was prepared in a single batch (50 mg per sample) and rehydrated in water for 10 min. The resin was washed twice with washing buffer (50 mM Tris–HCl pH 8) and resuspended to a 500 mg ml^{-1} slurry. Samples were added to 100 µl of resin slurry held in a spin column (Thermo Fisher Scientific, Waltham, MA, USA) and incubated for 2 h. The resin was washed with 500 µl of washing buffer containing 0.5% SDS and centrifuged, followed by washing buffer with 2 M NaCl, 80% acetonitrile (ACN) with 0.1% trifluoroacetic acid (TFA), and finally with washing buffer alone. The resin was resuspended in 500 µl of washing buffer, and 5 µg of Trypsin Gold (Promega, Madison, WI, USA) was added for on-resin digestion of cysteine-bound proteins. Samples were incubated for 16 h at room temperature, centrifuged to remove unbound peptides and washed following the previously outlined washing procedure. Bound cysteine-containing peptides were eluted from the resin twice using 250 µl of washing buffer with 50 mM DTT for 30 min and collected after centrifugation.

Peptide eluate was acidified with 25 µl of 5% TFA and desalted by solid-phase extraction (SPE) using 50 mg/1.0 ml Sep-Pak C18 cartridges (Waters Corp., Milford, MA, USA). Vacuum-dried peptides were dissolved in 50 µl of 0.1% TFA before LC-MS/MS analysis.

Global proteomics

An aliquot of each protein extract (100 µg) was reduced using 10 mM DTT for 30 min, alkylated with 30 mM IAM for 30 min, and precipitated with 1 ml of cold acetone. Samples were centrifuged and the protein pellet was resuspended in 100 µl of digestion buffer (50 mM Tris–HCl pH 8 and 2 M urea). Proteins were digested with 5 µg of Trypsin Gold (Promega) for 16 h at room temperature before quenching with 25 µl of 5% TFA. After desalting by SPE and vacuum centrifugation, samples were resuspended in 250 µl of 0.1% TFA before analysis.

LC-MS/MS analysis

Samples were analyzed using a NanoAcquity UPLC system (Waters) coupled to a TripleTOF 5600 mass spectrometer (AB Sciex, Framingham, MA, USA). Mobile phase A consisted of water with 0.1% formic acid and mobile phase B was ACN with 0.1% formic acid. Injections (5 µl) were made to a Symmetry C_{18} trap column (100 Å, 5 µm, 180 µm × 20 mm; Waters) with a flow rate of 5 µl min^{-1} for 3 min using 99.9% A and 0.1% B. Peptides were separated on an HSS T3 C_{18} column (100 Å, 1.8 µm, 75 µm × 250 mm; Waters) using a linear gradient to 35% mobile phase B over 90 min at a flow rate of 300 nl min^{-1}.

The mass spectrometer was operated in positive polarity and high-sensitivity mode. MS survey scans were accumulated across an m/z range of 350–1600 in 250 ms. For information-dependent acquisition, the mass spectrometer was set to automatically switch between MS and MS/MS experiments for the first 20 features above 150 counts having +2 to +5 charge state. Precursor ions were fragmented using rolling collision energy with an accumulation time of 85 ms. Dynamic exclusion for precursor m/z was set to an 8 s window. Automatic calibration was performed every 8 h using a tryptic digest of BSA protein standard to maintain high mass accuracy in both MS and MS/MS acquisition.

Database searching and label-free quantification

Acquired spectral files (*.wiff) were imported into PROGENESIS QI for proteomics (v.2.0; Nonlinear Dynamics, Northumberland, UK) according to settings described previously (McConnell *et al.*, 2018) and a combined peak list (*.mgf) was exported for peptide sequence determination and protein inference by MASCOT (v.2.5.1; Matrix Science, Boston, MA, USA). Database searching was performed against the UniProt reference proteome (39 196 canonical entries) for *A. thaliana*. Sequences for common laboratory contaminants (www.thegpm.org/cRAP; 116 entries) were appended to the database. Searches of MS/MS data used a trypsin protease specificity with the possibility of two missed cleavages, peptide/fragment mass tolerances of 15 ppm/0.1 Da, and variable modifications of acetylation at the protein N-terminus, carbamidomethylation at cysteine, deamidation at asparagine or glutamine and oxidation at methionine. For global proteomics, carbamidomethylation at cysteine was included as a fixed modification instead. Significant peptide identifications above the identity or homology threshold were adjusted to < 1% peptide false discovery rate (FDR) using the embedded PERCOLATOR algorithm (Käll *et al.*, 2007) and results (*.xml) were uploaded to Progenesis for peak matching. Identifications with a score < 13 were removed from consideration in Progenesis and, for global proteomics, relative quantification was performed using the Hi-N setting with up to three peptides and protein grouping employed. Results were then exported as 'Peptide Measurements' and 'Protein Measurements' from the 'Review Proteins' stage.

Statistical analysis of proteomics data

Data were processed using custom scripts written in R (v.3.5.1) as described previously (McConnell *et al.*, 2018). For the reversible oxidation analysis, the peptide measurements file was filtered for only sequences containing an unmodified cysteine residue (the absence of IAM modification on at least one cysteine in the sequence). Individual peptides were mapped to the intact

protein sequence to get the position(s) of unmodified cysteine sites and then represented as identifiers by joining the protein accession with the oxidized position(s). Matching identifiers were then grouped together by summing the abundance of contributing peptides. For global proteomics, the protein measurements file was filtered for proteins with more than two unique peptides. Because the oxidized-cysteine-containing peptides (i.e. identifiers) are measured on the peptide level and these peptides were not aggregated to form one protein measurement, a single peptide was sufficient for redox proteomics analysis.

Rows were removed if there was not at least one biological condition with 3/4 nonzero values across the Progenesis-normalized abundance columns. Values were $\log_2$-transformed and we applied a conditional imputation strategy using the IMP4P package (https://cran.r-project.org/web/packages/imp4p), where conditions with at least one nonzero value had missing values imputed using the impute.rand function with default parameters. For cases where a condition had only missing values, the impute.pa function was used to impute small numbers centered on the lower 2.5% of values in the data.

Statistical significance was determined using a two-tailed, equal variance *t*-test and *P*-values were adjusted for multiple comparisons with the method of Benjamini and Hochberg (Hochberg, 1995). Fold changes were calculated by the difference of the mean abundance values between conditions being compared. Only observations with FDR-adjusted $P < 0.05$ and $\log_2$-transformed fold change ≥ 1 or ≤ -1 were considered significantly different.

Results

Global and redox proteomics of WT and *agb1* following ABA treatment

To examine the role of reversible protein oxidative signaling in ABA responses as well as its dependence on functional G-proteins, both the global and redox proteomes of the WT plants were compared with the *agb1* mutants following 0 (control) and 2 h of ABA treatment (Fig. 1). Global proteomics quantified 9984 unique peptides corresponding to 1892 proteins (Supporting Information Table S1A). Of these, 261 exhibited significant changes in abundance following ABA treatment in WT plants, with 194 and 67 decreasing and increasing, respectively, mirroring our previous study on Arabidopsis roots (Alvarez *et al.*, 2011) (Fig. 2; Table S1B). Surprisingly, the *agb1* mutant showed a markedly diminished proteomic response to ABA compared to WT plants (Fig. 2b), with only 64 proteins showing significantly changed in abundance following ABA (46 decreasing and 18 increasing). Of the 261 changed proteins in the WT, 242 (93%) did not change in the *agb1* mutant, suggesting that the proteomic changes to ABA exposure are dependent on the presence of functional G-proteins. Only three and 10 proteins that exhibited increased and decreased abundance, respectively, in response to ABA were common between WT and *agb1* mutants. Furthermore, 45 (70%) proteins that were differentially abundant following ABA treatment in the *agb1* mutant did not change in the WT, indicating the existence of alternative ABA response mechanisms in the absence of functional G-proteins.

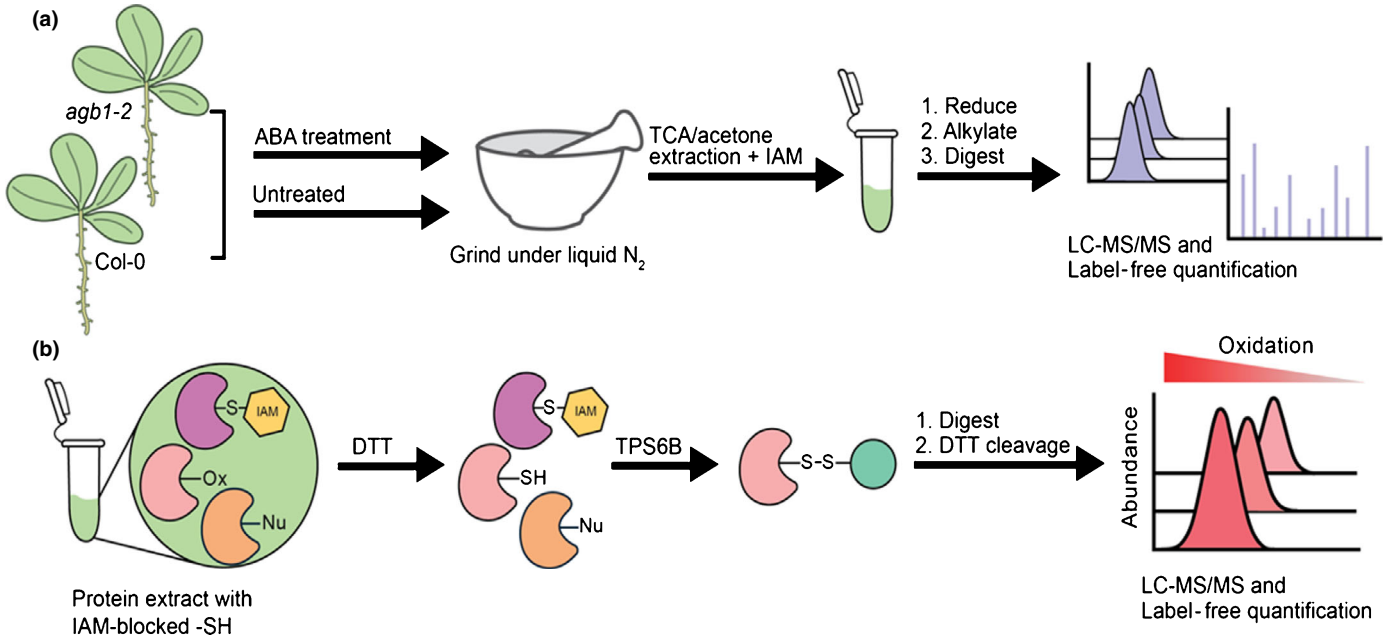

Fig. 1 Schematics of the experimental design of proteomics and redox proteomics analysis. (a) Wild-type (WT) and *agb1* null mutant seedlings of Arabidopsis were ground under liquid nitrogen, extracted via the trichloroacetic acid (TCA)/acetone method, and reduced thiols were blocked with iodoacetamide (IAM). Global proteomics analysis included reduction, alkylation and digestion of the lysate before analysis via MS-based label free quantitative (LFQ) proteomics. (b) For redox analysis, the lysate with blocked reduced cysteine thiols was reduced subsequently using dithiothreitol (DTT), therefore reducing all thiols that were reversibly oxidized *in vivo*. The lysate was then enriched for these now free thiols using TPS6B resin where they were bound, washed and digested on resin. The eluate was analyzed via LFQ proteomics.

(a)

Comparison	Total	Up	Down
WT-C vs WT-ABA	261	67	194
agb1-C vs *agb1*-ABA	64	18	46
WT-C vs *agb1-C*	161	39	122
WT-ABA vs agb1-ABA	79	43	36

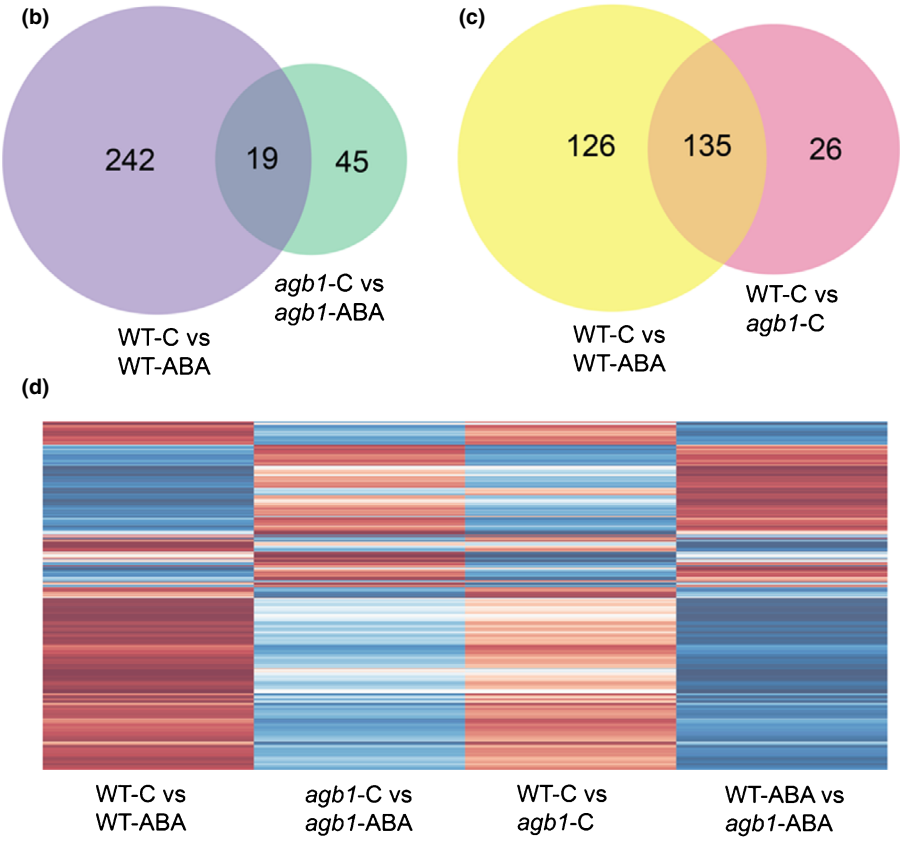

Fig. 2 Effects of abscisic acid (ABA) and the loss of AGB1 on the global proteome of Arabidopsis. (a) Number of proteins with significantly changed protein abundance in *agb1* and WT plants. (b) Venn diagram representing overlapping and unique differentially abundant proteins when comparing the ABA response in the WT and *agb1*. (c) Venn diagram representing overlapping and unique differentially abundant proteins when comparing the response of the WT to ABA and to the loss of *AGB1*. (d) Heatmaps of all differentially abundant proteins at the global proteome level in different comparisons. Red and blue indicate the $\log_2$ fold change value of increased and decreased protein levels, respectively.

The proteome of *agb1* was also inherently different from the WT with 161 proteins showing differential abundance (WT-C vs *agb1*-C). Surprisingly, these proteins showed substantial overlap with the ABA-responsive proteome of the WT (WT-C vs WT-ABA) plants (Fig. 2c,d; Table S1B), with 135 (84%) proteins overlapping between the two datasets. Of these, 37 showed opposite abundance changes; these proteins were more abundant in the WT plants in response to ABA treatment, but were inherently less abundant in the *agb1* mutants compared to the WT plants. This suggests that not only are the G-proteins required to fully execute the ABA response, but their absence also results in molecular phenotypes (i.e. proteomic changes) similar to those generated by ABA treatment (Fig. 2c,d). Thus, the lack of functional G-protein results in similar proteomic changes as exogenous stress treatment.

The PANTHER Overrepresentation Test (http://www.pantherdb.org) was used to determine the pathways most affected by ABA treatment with loss of G-proteins (Table S2). An analysis of Gene Ontology (GO) biological processes indicated that several categories related to primary metabolism, photosynthesis and several biotic and abiotic stresses were overrepresented in the WT plants in response to ABA but not in *agb1*. The mutant showed enrichment of the proteins involved in response to fungal pathogens, which was not observed in other comparisons (Table S2). Many of the categories overrepresented in the WT ABA-responsive proteome overlapped with the overrepresented categories caused by the loss of AGB1 (WT-C vs *agb1*-C, Table S2); however, the loss of AGB1 also showed enrichment of GO categories related to water deprivation, toxin metabolic processes (*c.* 18-fold) and hexose catabolic processes (*c.* 78-fold), which were not enriched in the ABA-responsive proteome. A comparison of GO categories in cellular components showed a significant enrichment of the proteasome pathway proteins and components (> 45-fold) in the ABA-responsive proteome of *agb1* mutants,

but not the WT plants (Table S2). Overall, these analyses suggest distinct effects of ABA on WT and *agb1* mutants, as well as an inherent effect of the loss of AGB1 on the Arabidopsis proteome.

To determine the role of oxidative signaling in ABA response networks and to assess the dependence of this response on AGB1, oxidized resin-assisted capture (OxRAC) was used to delineate the differential redox proteome following ABA treatment in WT and *agb1* (Fig. 1b). Across both genotypes, this method resulted in identification of 6891 unique oxidized cysteine-containing peptides, referred to as identifiers, derived from 3300 proteins (Table S3A), constituting the largest redoxome identified in plants to date (Ameztoy *et al.*, 2019; Huang *et al.*, 2019; McConnell *et al.*, 2019). Abscisic acid treatment in the WT resulted in 923 redox identifiers significantly changed in abundance, with 711 increasing and 212 decreasing (Fig. 3a; Table S3B). This corroborates that ABA induces an oxidative burst which probably acts as a signaling mechanism via modification of cysteine thiols (Watkins *et al.*, 2017; Ha *et al.*, 2018). The number of proteins mapping to oxidized cysteine-containing peptides (3300) is significantly higher than the total number of proteins (1892), as identification of oxidized proteins requires an enrichment step. This is also reflected in low overlap between these datasets. For example, of the 1018 unique proteins with differentially abundant oxidized cysteines, only 142 (*c.* 14%) are also differentially abundant in the global proteome (Table S3C).

The ABA-dependent redoxome of the *agb1* mutants was substantially different from the WT plants, with only 255 significantly changed redox identifiers (Fig. 3a). Mirroring the global proteomic analysis, 175 (69%) of the ABA-dependent differentially oxidized identifiers in the *agb1* mutants did not change in the WT. Furthermore, of the 80 protein identifiers that overlapped between the WT and *agb1* mutants in response to ABA (Fig. 3b), only 26 showed similar redox changes (Fig. 3d). These observations further establish that a functional G-protein complex is required for proper execution of ABA-dependent redox responses.

The substantially altered ABA-dependent redoxome of *agb1* prompted us to evaluate whether there are inherent differences in

(a)

Comparison	Total	Up	Down
WT-C vs WT-ABA	923	711	212
agb1-C vs *agb1*-ABA	255	128	127
WT-C vs *agb1-C*	688	481	207
WT-ABA vs agb1-ABA	218	104	114

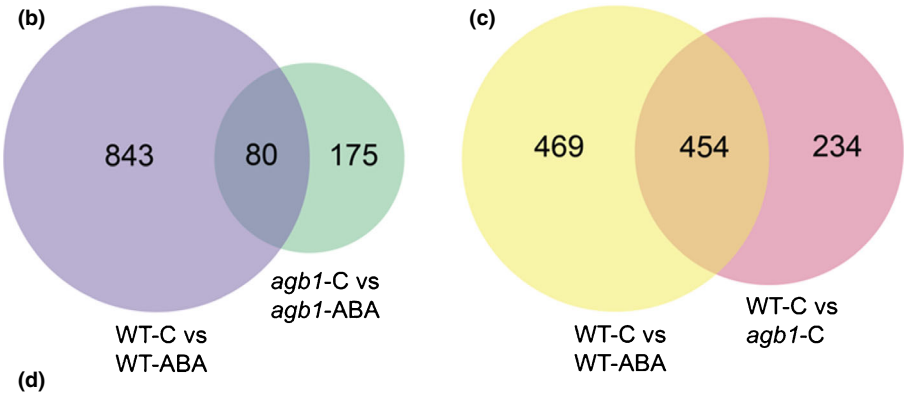

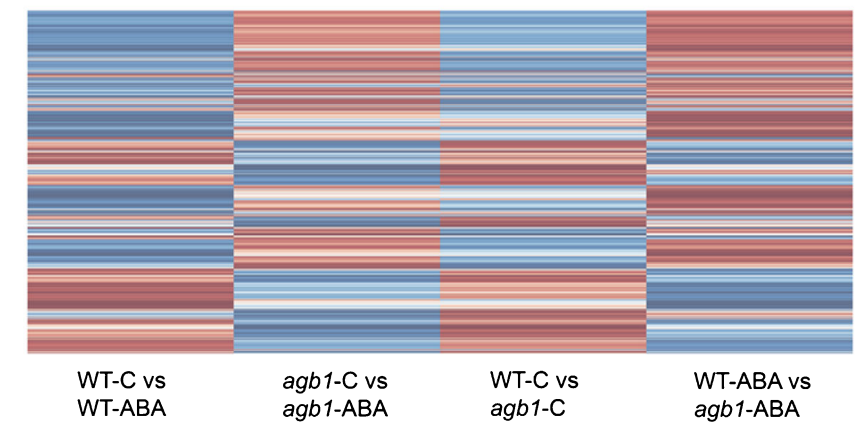

Fig. 3 Effects of abscisic acid (ABA) and the loss of *AGB1* on the redox proteome of Arabidopsis. (a) Number of peptides with significantly changed oxidation of cysteine thiols in *agb1* and WT plants. (b) Venn diagram representing overlapping and unique differentially oxidized proteins when comparing the ABA response in the WT and *agb1*. (c) Venn diagram representing overlapping and unique differentially oxidized proteins when comparing the response of the WT to ABA and to the loss of *AGB1*. (d) Heatmaps of all differentially oxidized peptides at the redox proteome level in different comparisons. Red and blue indicate the $\log_2$ fold change value of increased and decreased cysteine oxidation, respectively.

its redox status compared to the WT plants. Under control conditions, *agb1* revealed a significantly different oxidative state than that of the WT, with 481 identifiers increased and 207 decreased (Fig. 3a; Table S3A). These 688 differential identifiers were derived from 564 unique proteins, many not known to be oxidized. Similar to what was seen at the total proteome level, *c.* 75% of the identifiers exhibiting higher oxidation and 42% of the identifiers exhibiting lower oxidation were common between WT plants treated with ABA or the plants lacking a functional AGB1 (Fig. 3c). Only two identifiers exhibited opposite trends between these comparisons. A mitogen-activated protein kinase 14 (MAPK14) showed significant ABA-dependent higher oxidation in WT plants, but lower oxidation due to the loss of AGB1. Conversely, a small acidic protein, thionin 2, which is involved in the defense response, showed *c.* 5-fold lower oxidation in WT plants due to ABA treatment, but higher oxidation in *agb1* mutants under control conditions. Oxidation changes specific to *agb1* mutants were also detected, with 118 protein identifiers showing higher and 119 showing lower oxidation compared to the WT plants. These data suggest that AGB1 plays a significant role in maintaining the overall basal redox status in plants.

Functional categorization of ABA- and G protein-dependent redoxome

The ABA- and G-protein-dependent redoxome revealed that the differentially oxidized proteins span multiple cellular localizations (Table S4). In each of the major cellular components, the redox proteome of *agb1* was substantially different from that of the WT plants, as visualized via density plots (Fig. 4). The WT experiences a higher density of increased oxidation than *agb1*, whereas *agb1* experiences a higher density in decreased oxidation regardless of localization.

An analysis by the PANTHER overrepresentation test corroborated these observations. Many enriched protein categories were common to the ABA-responsive redox proteome of the WT plants and the redox changes due to the loss of *AGB1* (Fig. 3; Table S4). Gene Ontology analysis of biological processes revealed an overrepresentation of proteins related to multiple primary and secondary metabolic processes in the WT plants in response to ABA that were not enriched in the *agb1* mutant plants following ABA treatment (Table S4A).

Gene Ontology analysis of molecular functions showed nearly no overlap between ABA-responsive, differentially oxidized protein categories between the WT and *agb1* mutants, although a substantial overlap was seen between ABA-treated WT plants (WT-C vs WT-ABA) and due to the loss of *AGB1* (WT-C vs *agb1*-C), representing proteins with transferase, dehydrogenase and ligase activities among others (Table S4B). The *agb1* mutants showed an enrichment of pentosyltransferase activity (*c.* 16-fold), which was not seen in other comparisons. A significant enrichment in oxidoreductase activity was also seen in the ABA-treated WT plants and due to the loss of AGB1, which is not surprising due to the known reliance of oxidoreductases on cysteine thiol oxidation (Couturier *et al.*, 2013). Interestingly, the ABA-treated WT plants showed an enrichment of oxidoreductases that acted on CH-OH donors, whereas those due to AGB1 loss acted on the sulfur group of donors (Table S4B).

Using a combination of KEGG analysis, GO enrichment and Uniprot annotations, the significantly changed identifiers were manually annotated into several broad categories, which show the major effect of ABA and G-proteins on key metabolic and cellular energetics processes (Table S5). The differentially oxidized proteins were also mapped using the PATHVIEW mapping tool of KEGG.

Reversible oxidation across stress responsive proteins A total of 191 protein identifiers derived from 141 stress-responsive proteins exhibited differential oxidation, with WT plants showing differential oxidation across 90 proteins (120 identifiers). The

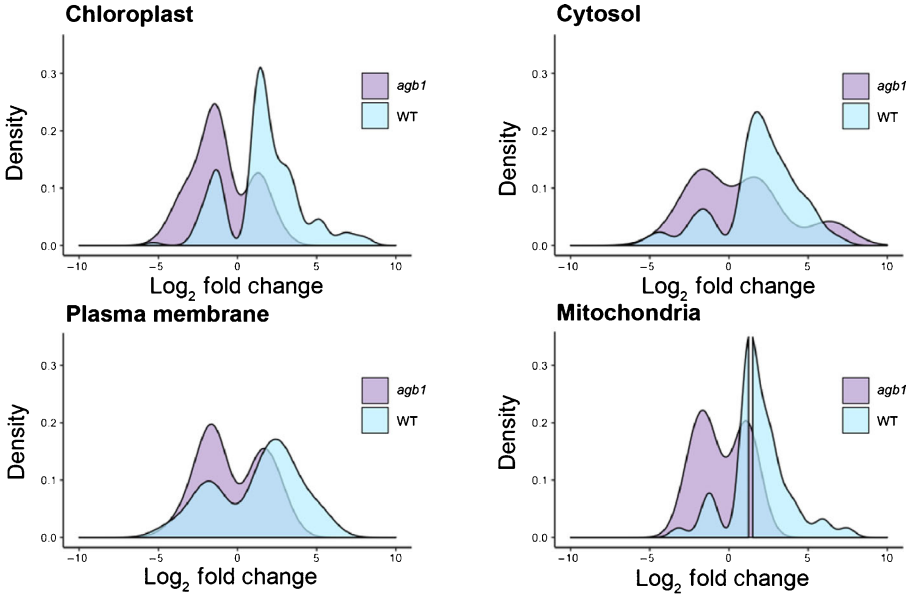

Fig. 4 Density plots depicting significant oxidation changes in different cellular compartments. Oxidation changes in the WT and *agb1* following abscisic acid (ABA) treatment in the chloroplast, cytosol, plasma membrane and mitochondria. The *x*-axis indicates the magnitude of increase or decrease in oxidation, expressed as $\log_2$ fold change. The *y*-axis indicates the accumulation of differentially oxidized identifiers. The density plots indicate that the WT has an increased accumulation of cysteine oxidation throughout cellular compartments.

oxidation status of ABA-responsive proteins was significantly different in *agb1*, with only 48 protein identifiers exhibiting altered oxidation (Table S5A). Moreover, as seen at the whole redoxome level, many ABA-responsive proteins exhibiting altered oxidation in the WT were inherently differentially oxidized in the *agb1*. These included known markers of ABA signaling, dehydration stress, osmotic stress and salt stress. Corroborating these observations, the *agb1* mutants exhibited altered sensitivity to exogenous ABA during seed germination. The *agb1* mutant seeds showed reduced germination in the presence of 0.1–2 μM exogenous ABA, which was different from the WT seeds. In the presence of 1 μM exogenous ABA, *c.* 35% and 65% inhibition of seed germination was observed for WT and *agb1* mutant seeds, respectively, at 48 h postimbibition (Fig. 5a). The *agb1* mutants also showed a significantly higher anthocyanin index, another measure of stress response, both inherently and in response to dehydration (Fig. 5b).

Defense response-related proteins also experienced major changes in oxidation, constituting almost half of all proteins identified in stress-responsive categories. These corroborate the role of ABA and G-proteins during pathogenesis and the immune response in plants (Ton *et al.*, 2009; Nitta *et al.*, 2015). The defense-related redoxome of the WT was distinct from the *agb1* mutants and several protein identifiers from *agb1* mutants without ABA treatment (WT-C vs *agb1*-C) showed similar oxidation changes as the ABA-treated WT plants, as shown for a subset of proteins that were mapped using the PATHVIEW mapping tool (Fig. S1) (Luo *et al.*, 2017).

A large number of proteins implicated in the oxidative stress response were also identified. Unsurprisingly, these proteins were represented by identifiers largely increasing in oxidation, with 30 identifiers denoting increased oxidation and six identifiers denoting decreased oxidation. Of these, 16 identifiers were derived from 12 proteins that are directly involved in ROS mitigation. These include several peroxidases, which showed some of the largest changes in oxidation. Importantly, all these peroxidases exhibited altered oxidation levels between ABA-treated WT and *agb1* mutant plants (Fig. 5c). In addition to ROS quenchers, enzymes that propagate oxidative signaling via the oxidation of methionine and cysteine residues were also differentially oxidized following ABA treatment in the WT. This is illustrated through several family members of both methionine sulfoxide reductase and thioredoxin (Fig. 5d). Proteins involved in glutathione metabolism, peroxisome metabolism and fatty acid degradation (Figs S2–S4) followed similar patterns, where significant changes in oxidation level were observed in the WT plants in response to ABA, which overlapped with the changes observed due to the loss of AGB1. Many of these were not observed in the *agb1* mutants in response to ABA, confirming the requirement of a functional G-protein for these pathways to be active. In agreement with these data, *agb1* showed higher ROS accumulation than WT plants under control conditions and under ABA treatment (Fig. 5e,f). While these data may appear counterintuitive, given fewer redox identifiers in the *agb1* mutants compared to the WT plants, it is likely to be due to the fact that the *agb1* mutants already accumulate more ROS, even without ABA treatment. Therefore, when treated with additional ABA, we do not see more redox changes. Additionally, these redox proteomics experiments identify targets of reversible oxidative signaling; an inherently increased ROS level in *agb1* mutants may cause irreversible oxidative damage on protein residues that will not be reflected in the number of quantified identifiers.

Reversible oxidation of photosynthesis-related proteins The photosynthetic electron transport chain (pETC) and chloroplastic NADPH oxidase provide the integral ROS needed for stomatal responses following ABA exposure (Foyer & Noctor, 2003; Iwai *et al.*, 2019). Abscisic acid treatment in the WT resulted in 28 photosynthesis-related proteins, including 26 identifiers with increased oxidation and nine identifiers with decreased oxidation (Table S5B). By contrast, ABA perturbed oxidation of only nine identifiers from photosynthetic proteins in *agb1*, of which two overlapped with the WT and showed similar changes. Similar to what was observed for stress responsive proteins, the photosynthesis-related ABA-dependent redox modified identifiers showed major overlap with the identifiers showing differential oxidation due to the loss of functional AGB1 (Fig. S5).

The largest increase in oxidation occurred on several Chl biosynthesis enzymes such as HEMA1 (Brzezowski *et al.*, 2015), Mg-chelatase CHLI (Eckhardt *et al.*, 2004) and GUN4, which directly binds to Mg-chelatase to stimulate activity. Eight identifiers on seven proteins related to photosynthetic electron transfer were also differentially oxidized in the WT following ABA exposure. The largest change in oxidation was observed on subunit X of photosystem I (PsaK), which also showed higher oxidation due to the loss of AGB1. Lhca2 likewise increased in oxidation, but only in WT, ABA-treated plants. Outside of PsaK, three other subunits along the integral pETC had identifiers with differential oxidation, cytochrome *f* (PetA), the Fe–S subunit of cytochrome b_6f (PetC) and photosystem II (PSII) subunit T (PsbT). Neither PetC nor PetA were differentially oxidized in the nontreated *agb1* mutant compared to the WT or in the ABA-treated *agb1* (Fig. S5).

Abscisic acid-responsive oxidative changes on proteins responsible for functions related to chloroplastic and photosynthetic damage repair were also observed. Differential oxidation occurred across 10 identifiers of six proteins, with the largest increase in oxidation occurring on low PSII accumulation 3 (LPA3), followed by high Chl fluorescence phenotype 244 (HCF244), both of which are involved in PSII repair (Lu, 2016; Li *et al.*, 2019). Many of these oxidized cysteines were also differentially oxidized in *agb1*, but only when comparing the basal level of oxidation with that of the non-ABA-exposed WT. In addition, thylakoid formation 1 (THF1), which is involved in thylakoid biogenesis and G-protein-dependent glucose signaling (Huang *et al.*, 2006), was also highly oxidized.

To corroborate the redox proteomics data, we measured the photosynthetic efficiency of the WT and *agb1* mutants, in response to dehydration stress (as a proxy for ABA). The *agb1* mutants exhibited inherently distinct photosynthetic efficiency, in part due to their higher stomatal density. However, a comparison of dehydration-dependent changes across two genotypes showed

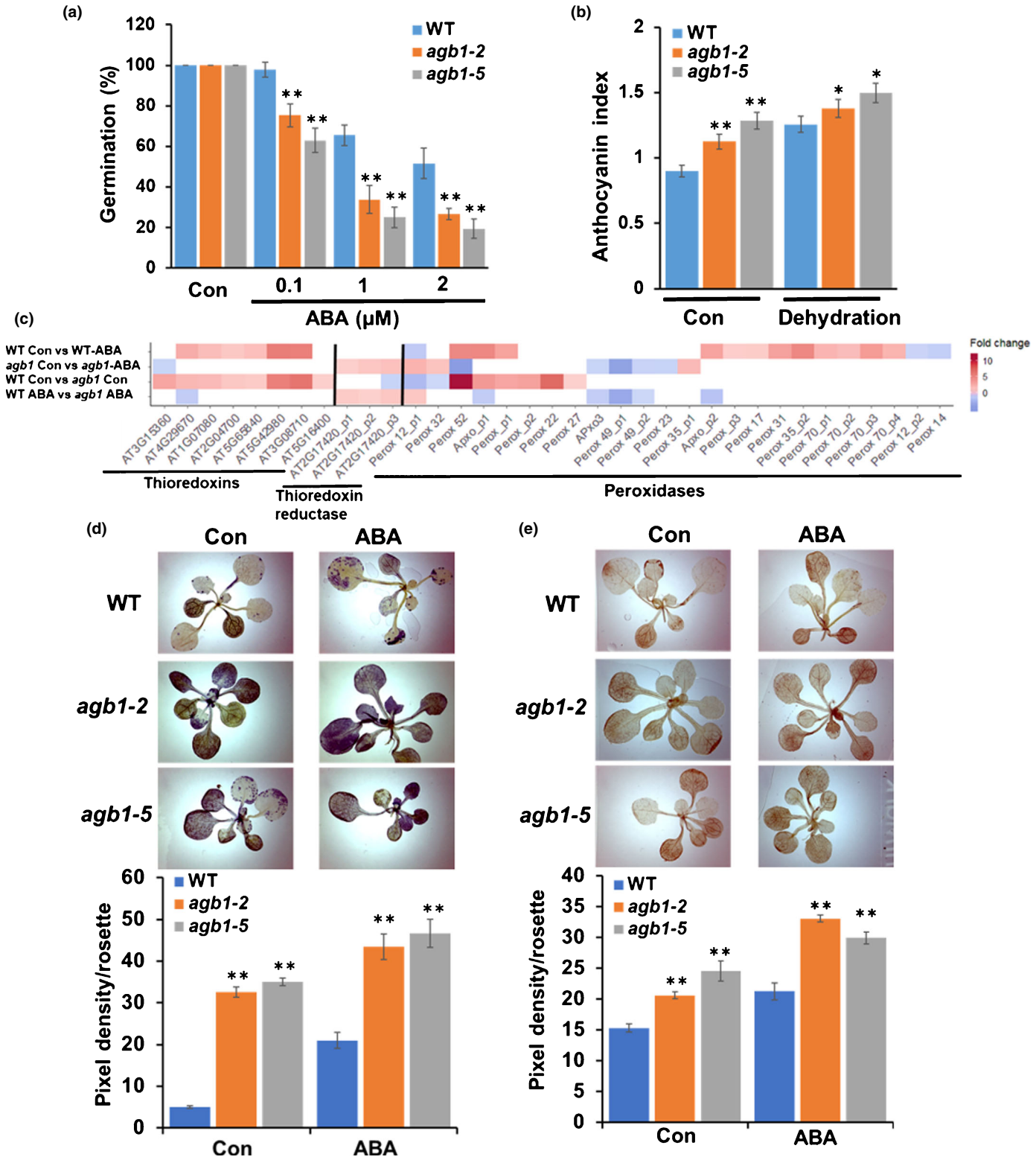

Fig. 5 Effect of abscisic acid (ABA) on *agb1* mutants. (a) *agb1* mutants are hypersensitive to ABA for inhibition of germination compared to the WT. (b) *agb1* mutants show a higher anthocyanin index in response to dehydration compared to the WT. (c) ABA-dependent oxidation changes in all peroxidases identified in this study are distinct in WT vs *agb1* mutants. *agb1* mutants show reduced or no change in oxidation of thioredoxins, but higher oxidation of thioredoxin reductase identified in this study. *agb1* mutants show higher reactive oxygen species (ROS) levels compared to WT plants, inherently and in response to ABA, as measured by (d) nitroblue tetrazolium (NBT) staining and (e) 3,3′-diaminobenzidine (DAB) staining. Top, representative images, bottom, quantification of NBT and DAB staining, $n = 4$. Error bars represent ±SE. Asterisks in (a, b, d, e) represent significant differences: *, $P < 0.05$ and **, $P < 0.01$ using Student's *t*-test.

significant differences in their photosynthetic efficiency, NPQ and ETRs, thus showing an altered photosynthetic response following increased ABA levels in the WT compared to *agb1* (Fig. 6). These alterations suggest an essential function for AGB1-mediated reversible cysteine oxidation across the photosynthetic apparatus.

Reversible oxidation of proteins related to sugar and carbohydrate metabolism Abscisic acid signaling has been linked to large-scale reorganization of carbohydrate metabolism in Arabidopsis (Kempa *et al.*, 2008; Thalmann *et al.*, 2016). We identified 79 differentially oxidized identifiers (62 higher and 17 lower oxidation) from 69 proteins involved in carbohydrate metabolism in WT plants in response to ABA (Table S5C). This suggests that reversible oxidation is an essential regulator of carbohydrate metabolism in response to ABA. Moreover, 76 of these identifiers did not experience differential changes in the *agb1* mutant following treatment. As was observed with other metabolic processes, many of the identifiers showed inherently differential oxidation in the nontreated *agb1*, suggesting that maintaining the intracellular redox state in basal conditions is dependent on functional AGB1 (Fig. 7a).

Of the increased differentially abundant identifiers, 14 belonged to enzymes involved in starch biosynthesis and degradation. Starch synthase enzymes AtSS5 and AtSS2 had some of the highest increases in oxidation in the WT in response to ABA and in the nontreated *agb1* mutants. Starch staining of WT and *agb1* mutant leaves under control and ABA-treated conditions confirmed these observations and showed inherent differences in the starch content of the mutant as well as an effect of ABA treatment on WT and mutant plants (Fig. 7b).

Abscisic acid treatment of the WT or the loss of *AGB1* also caused significant and overlapping changes in cysteine oxidation on proteins involved in glycolysis, gluconeogenesis and pentose phosphate pathway (Figs S6, S7), including quantification of several newly identified oxidation sites. Only two identifiers involved in glycolysis/gluconeogenesis decreased in oxidation upon ABA treatment; triose phosphate isomerase (TIM) in both the WT and *agb1* and glyceraldehyde-3-phosphate dehydrogenase C2 (GAPC2) only in the WT. TIM is regulated via *S*-glutathionylation and *S*-nitrosylation on C127 and C218, but redox modifications on C186 have not been previously reported (Dumont *et al.*, 2016). By contrast, GAPC2 modifications C156 and C160 have been characterized to delineate both glutathionylation and nitrosylation, and have been shown to decrease in activity following exogenous oxidation (Bedhomme *et al.*, 2012). It is hypothesized that GAPC2 and TIM function in concert to regulate metabolic flux under stress conditions and that the flux of starch biosynthesis is both ABA- and G-protein-dependent (Dumont & Rivoal, 2019).

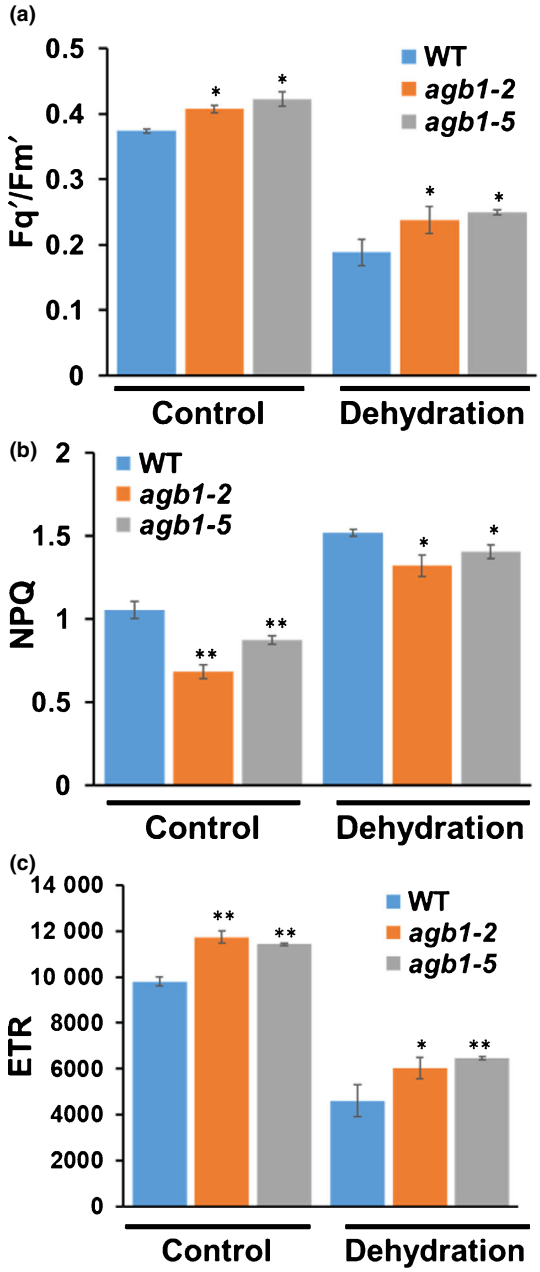

Fig. 6 AGB1 has a role in regulation of photosynthesis during dehydration stress. Multiple photosynthetic parameters were quantified in WT, *agb1-2* and *agb1-5* plants under control (Con) and 4 h of dehydration treatment using the Phenovation CropReporter. (a) F'_q/F'_m (operating efficiency of PSII), (b) nonphotochemical quenching (NPQ) and (c) electron transfer rate (ETR), of *agb1* relative to WT plants under control and dehydration stress conditions are shown. Data represent the mean and standard errors (±SE) ($n = 3$) of one of the two independent experiments with similar results. Asterisks represent significant differences: *, $P < 0.05$ and **, $P < 0.01$ using Student's *t*-test.

ABA- and G-protein-dependent reversible oxidation of mitochondrial energy metabolism Mitochondria are second only to chloroplasts in the propensity for organelles to produce ROS, and have been specifically shown to generate ROS as a second messenger following ABA exposure (He *et al.*, 2012; Huang *et al.*, 2016). The proteins related to oxidative phosphorylation showed some of the most distinct differences between the WT and *agb1* mutants (Fig. S8). In the WT, ABA treatment caused differential oxidation of 24 identifiers, 21 of which increased in oxidation, deriving from 16 mitochondrial proteins (Table S5D). All but three of these identifiers are from proteins that directly participate in electron transfer via the mitochondrial

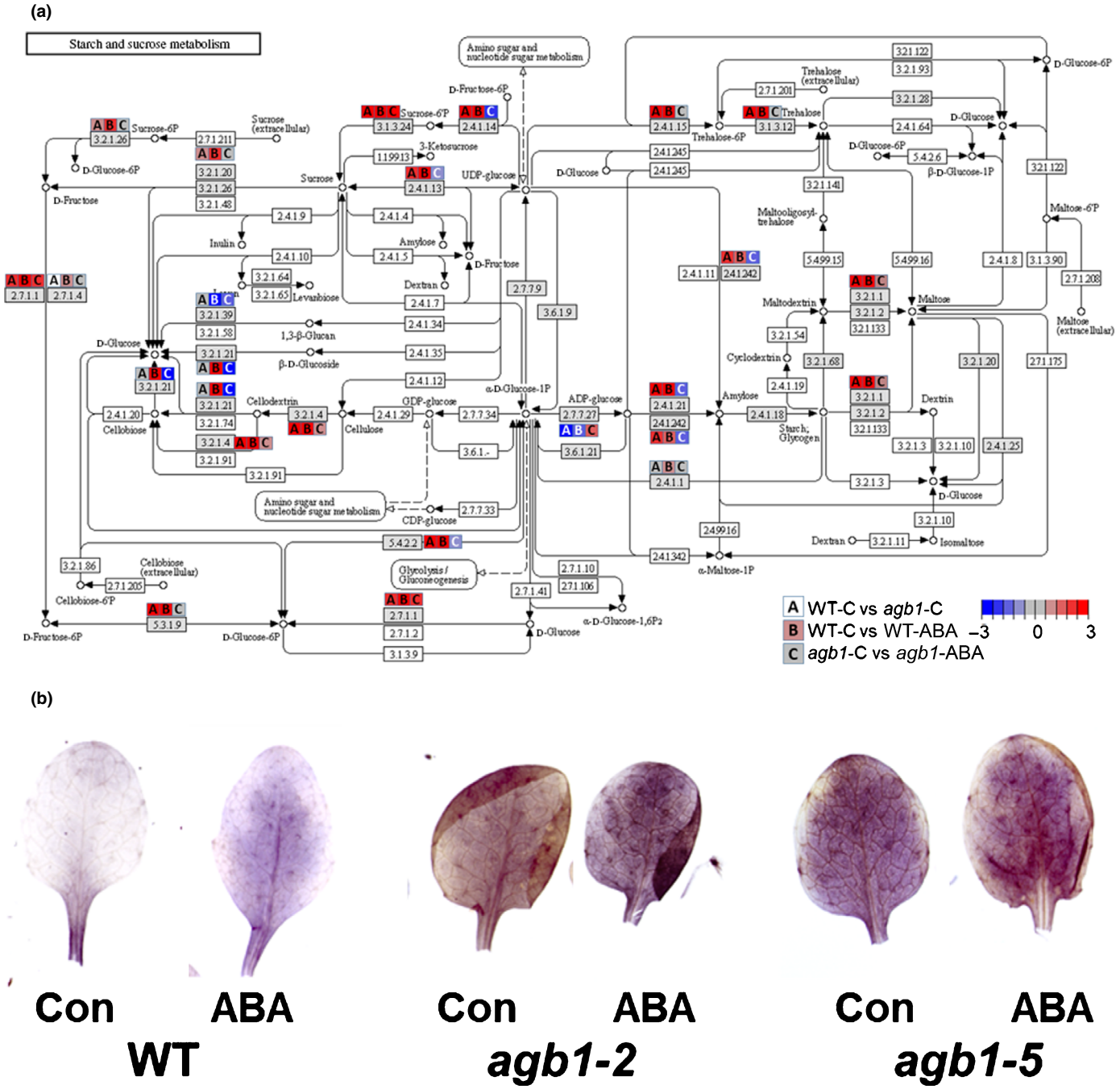

Fig. 7 Effect of abscisic acid (ABA) and *agb1* on starch and sucrose metabolism. (a) KEGG pathways related to starch and sucrose metabolism were visualized using Pathview mapping tools. Dashed lines show links to connecting pathways. Red and blue show increased and decreased oxidation, respectively. Letters A, B and C included in the color-coded fold changes refer to the oxidation level of a particular protein in different comparisons. (b) WT and *agb1* mutant leaves were stained for starch content using Lugol's solution under control conditions and ABA treatment.

electron transport chain (mtETC). None of these changed in the *agb1* mutants in response to ABA, although five identifiers showed inherently higher oxidation in the *agb1* mutants. Most identifiers came from ATP synthase with eight showing increased oxidation and one showing decreased oxidation, with oxidation occurring across both F- and V-type proteins.

Succinate dehydrogenase (SDH-1), an essential component both in the mtETC as well as the TCA cycle, exhibited an ABA- and G-protein-dependent increase in oxidation on several cysteines, including C526 that has previously been shown to undergo *S*-nitrosylation. SDH-1 is a component in the thioredoxin regulatory system (Fares *et al.*, 2011) and has been shown to be essential in the proliferation of ROS (Gleason *et al.*, 2011). Incidentally, ABA-mediated reversible oxidation of SDH-1 has also been reported in *Brassica napus* (Zhu *et al.*, 2014). Further targeted studies would help delineate the redox dependence of

SDH-1 and its roles in both electron transfer and carbohydrate synthesis.

MAPK14 may act as a direct target of AGB1 in redox signaling We identified MAPK14 as one of the proteins oxidized in an AGB1-dependent manner. MAPKs are known downstream effectors of G-proteins in many eukaryotes (Sanchez-Fernandez *et al.*, 2014; Xu *et al.*, 2015; Alvaro & Thorner, 2016; Yuan *et al.*, 2017). To elucidate a functional connection, we analyzed the mutants lacking the *MAPK14* gene (*mapk14-1* and *mapk14-2*) for physiological traits that differ between the WT and *agb1* mutants. The overall plant phenotype of the *mapk14* mutants was indistinguishable from the WT plants (Fig. S9A) and the *mapk14* mutant seeds germinated with similar efficiency as the WT seeds in the presence of exogenous ABA (Fig. S9B). The general photosynthetic parameters of the *mapk14* mutants were also similar to the WT plants under both control and dehydration stress conditions (Fig. S9C–E). However, the mutants showed higher accumulation of ROS under both control conditions and ABA treatment, similar to what was observed for the *agb1* mutants (Fig. 8a,b). The anthocyanin index of *mapk14* mutants was similar to WT plants under control conditions, but was significantly higher that WT plants after dehydration (Fig. 8c), suggesting their altered response to exogenous stresses.

Discussion

Levels of transcripts, proteins and metabolites are carefully and dynamically controlled to ensure proper plant adaptive responses (Takahashi *et al.*, 2018; van der Reest *et al.*, 2018; Cimini *et al.*, 2019; Mergner *et al.*, 2020). The proteins are not only affected in their overall abundance, but also at the level of multiple post-translational modifications that have critical roles in controlling their stability, activity and function (Liu *et al.*, 2014; McConnell *et al.*, 2019; Mergner *et al.*, 2020; Smythers & Hicks, 2021). Exposure to various abiotic stresses leads to generation of ROS (Zandalinas *et al.*, 2018; Xu *et al.*, 2019), which then proliferate signaling across protein pathways through reversible oxidation of

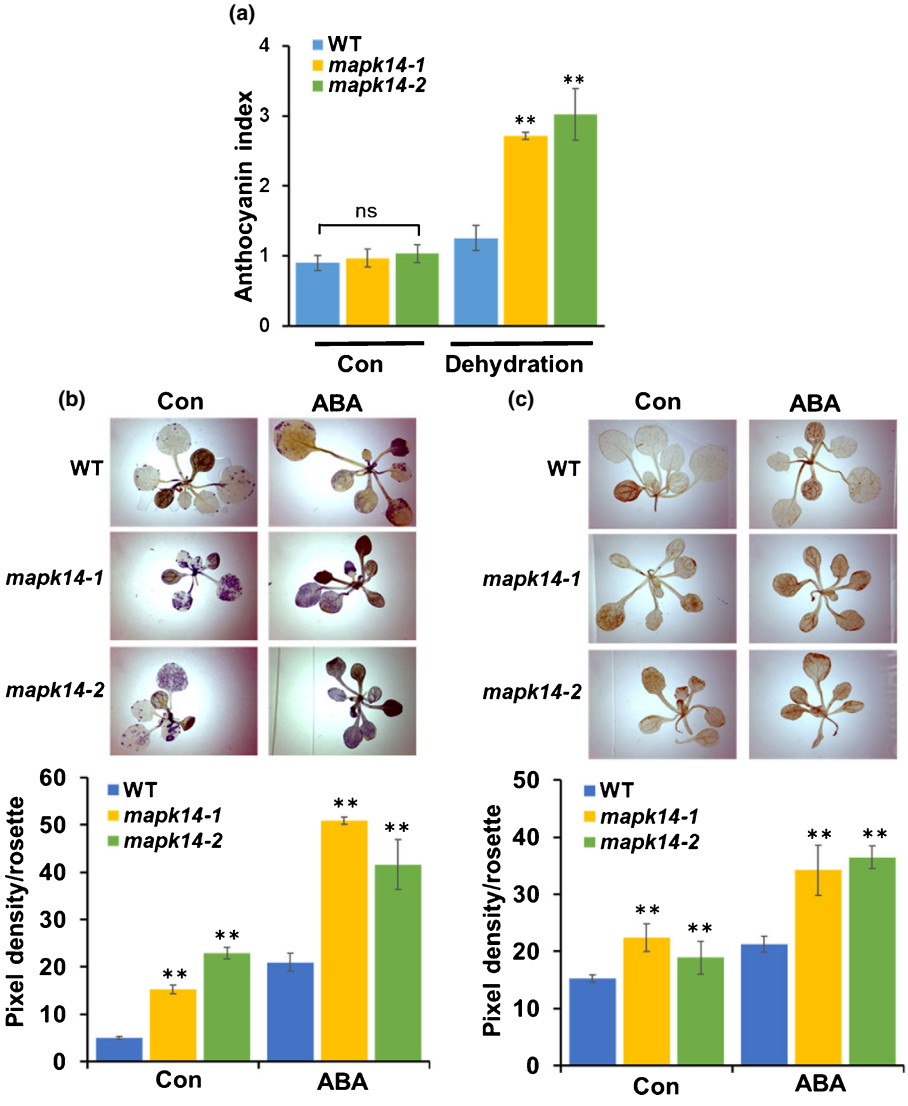

Fig. 8 *mapk14* mutants show altered stress responses. (a) *mapk14* mutants have a higher anthocyanin index in response to dehydration compared to WT plants. *mapk14* mutants show higher reactive oxygen species (ROS) levels compared to WT plants, inherently and in response to abscisic acid (ABA), as measured by (b) nitroblue tetrazolium (NBT) staining and (c) 3,3′-diaminobenzidine (DAB) staining. Top, representative images, bottom quantification of NBT and DAB staining, $n = 4$. Vertical lines in some of the images are the edges of coverslips/slides. Error bars represent ±SE. Asterisks represent significant differences: **, $P < 0.01$ using Student's *t*-test; ns, nonsignificant difference.

cysteine thiols, resulting in sulfenylation, nitrosylation and glutathionylation, among others (Liu *et al.*, 2014; van der Reest *et al.*, 2018; Ameztoy *et al.*, 2019; McConnell *et al.*, 2019). While ABA has been previously shown to exert redox changes in plants (Choudhury *et al.*, 2017; Mittler, 2017; Xu *et al.*, 2019), its effects have been mostly analyzed in the context of a few proteins without a comprehensive analysis of how it might affect the overall redox status of the proteome. Therefore, guided by an established connection between ABA, redox changes and G-proteins (Alvarez *et al.*, 2013; Liu & He, 2016; Liu *et al.*, 2017), we aimed to elucidate the interrelationship between them at the global and redox proteome levels. We report one of the largest plant redox proteomes identified to date (Liu *et al.*, 2014; Slade *et al.*, 2015; Ameztoy *et al.*, 2019; Huang *et al.*, 2019; McConnell *et al.*, 2019), by site-specific mapping and quantification of 6891 oxidized-cysteine sites on 3300 proteins (Figs 2–4; Tables S1–S4). Abscisic acid-dependent protein abundance changes as well as redox changes were significantly compromised in the *agb1* mutants (Figs 2, 3), implying that a functional G-protein signaling system is required to transduce ABA/stress-related cues.

G-proteins and ABA have overlapping roles in cellular redox regulation

One of the most significant findings from these analyses is the surprisingly similar oxidative changes due to the exogenous ABA treatment and the loss of G-protein function (Figs 5–7). Although G-proteins have long been identified as key regulators of plant stress responses (Pandey, 2019), the details of their signaling mechanisms remain unclear. This study establishes that the loss of G-protein function in plants dramatically shifts the redox environment of the cell, as shown through overlapping patterns of oxidative changes in multiple protein categories between the ABA-treated WT and the *agb1* plants (Tables S3, S5). Furthermore, several proteins across varied pathways including ROS response, carbohydrate metabolism and photosynthesis were dependent on AGB1 for oxidative regulation, indicating that the proliferation of redox-related G-protein signaling extends throughout cellular metabolic pathways (Table S5). These data corroborate that G-proteins are required for plants' optimal response to ABA and may also explain the reported and observed (Fig. 5) altered sensitivity of G-protein mutants to various abiotic stresses (Urano *et al.*, 2016; Roy Choudhury *et al.*, 2020).

This study also suggests a relatively direct role of G-proteins in redox regulation via the control of thioredoxin (TRX) proteins, an important component of a plant's thiol redox regulatory machinery (Fig. 5). Moreover, the magnitude of differential oxidation both in response to ABA as well as due to AGB1 loss suggests a circuitry of redox regulation that is exceedingly complex, with several proteins dependent on both ABA and AGB1. For example, GSTU17 increased in oxidation following ABA treatment in the WT, but experienced no difference in *agb1*. GSTU17 is a known negative regulator of ABA signaling in plants; by decreasing the intracellular glutathione pool, GSTU17 inhibits ABA signaling during periods of ideal growth (Chen *et al.*, 2012). However, GSTU17 expression is also decreased following exogenous ABA application and increased under osmotic stress, showing diverging signaling processes (Wu *et al.*, 2020). Since the oxidation of GSTU17 following ABA exposure is clearly AGB1-dependent, this suggests an interdependency between G-protein-, ABA-, redox- and glutathione-mediated signaling to exquisitely coordinate the redox state in response to changing stress conditions. We also identified an MAPK14 which is oxidized in an AGB1-dependent manner. Physiological experiments performed with the mutant plants lacking *MAPK14* gene showed that a subset of AGB1-mediated responses are altered in these mutants (Fig. 8), suggesting that this MAPK could be a direct downstream target of AGB1 for redox responses. Incidentally, a recent study reported the role of MAPK14 in auxin-dependent lateral root formation (Lv *et al.*, 2021), a plant phenotype known to be regulated by AGB1 (Ullah *et al.*, 2003).

ABA-generated carbohydrate flux is mediated by redox signaling

Enzymes related to starch degradation have been experimentally shown to be regulated via redox mechanisms, with many degradation proteins activated by the reducing conditions found in low-light conditions, thus enabling plant cells to rapidly mobilize energy stores during periods of low photosynthetic flux (Santelia *et al.*, 2015). However, following ABA exposure, the exceedingly elevated oxidation of biosynthesis-related enzymes suggests that ABA uses ROS-mediated signaling to decrease the activity of synthetic enzymes while simultaneously increasing the activity of degradative components. Both AtSS5 and AtSS2 experienced large increases in oxidation (Table S5). Despite lacking glycosyltransferase activity, the noncanonical starch synthase isoform AtSS5 promotes the initiation of chloroplast-localized starch granules by providing a binding site for both glucans and myosine-resembling chloroplast proteins (Abt *et al.*, 2020). By contrast, AtSS2 enzymatically elongates intermediate-length glucan chains during the formation of starch granules and is regulated by phosphorylation from chloroplast casein kinases (CKII) (Commuri & Keeling, 2001; Patterson *et al.*, 2018). In response to oxidative stress, maltose is released from starch and metabolized into sucrose, which can then scavenge ROS in the cytosol (Thalmann *et al.*, 2016). The increase in cysteine oxidation on both AtSS5 and AtSS2 may therefore be a sensor that diminishes starch synthesis in favor of degradative processes. Our analysis identified a key role of G-proteins in this process, which was confirmed by physiological assays (Fig. 7).

Reversible cysteine oxidation primes bioenergetic pathways for stress induction

Abscisic acid exposure in plants has been shown to have minimal effects on the overall efficiency of photosynthesis, potentially due to its ability to shift energy resources away from those needed to increase growth and toward processes related to metabolic maintenance (Franks & Farquhar, 2001; Yoshida *et al.*, 2019). The increased oxidation across cysteine thiols on subunits of

V-ATPase, which has been previously shown to accumulate disulfide bonds under stress to downregulate activity, could correlate with a decreased flux of ATP production following ABA exposure as bioenergetic pathways reallocate resources toward metabolic maintenance (Feng & Forgac, 1994; Tavakoli *et al.*, 2001; Seidel *et al.*, 2012). Similarly, unlike the overoxidation that results in protein degradation, the increased cysteine oxidation of pETC proteins such as PetC, PetA and PsnB3 probably confers stability and/or protection (Foyer, 2018). These proteins are important regulators of electron flow, with variations in regulation leading to cyclic electron flow that avoids counterregulation by the well-characterized proton gradient regulation 5 pathway (Jin *et al.*, 2017). While oxidative regulation of PetC, PetA and PsnB3 is not surprising due to their Fe–S subunits, these proteins have not previously been linked to ABA or G-protein signaling. Similarly, the previously described oxidation increase on photorepair proteins LPA3 and HCF244 only occurred in the WT following ABA treatment, further connecting AGB1 with photosynthetic regulation, this time by way of repair pathways.

Collectively, our analysis identified an array of signaling, metabolic and regulatory proteins that can undergo redox-dependent modification in response to stress (Table S5; Figs 7, S1–S8). Such nontargeted studies are necessary to identify new pathways, proteins and networks which may not be obvious when performing targeted functional analysis. It also showed an extensive and similar effect of exogenous stress and the loss of G-protein function on plants on processes as fundamental as photosynthesis, redox balance and energetics, corroborating the roles of G-proteins in adjusting optimal plant growth under any given environment. This implies that the loss of key proteins (e.g. AGB1), which have been established to have pleotropic effects, appear to modulate not just one specific pathway or protein, but probably something at the fundamental level (e.g. redox changes), which is eventually manifested as different phenotypes. Furthermore, in the particular example presented in this study, the loss of functional G-protein complexes is perceived as 'stress' by plants, similar to what is caused by ABA. This explains why plants lacking different G-proteins are more sensitive to nonoptimal growth conditions, as these are already not in their ideal physiological state.

Acknowledgements

Research in the Pandey lab is supported by the National Science Foundation grants (IOS-1557942 and MCB-1714693) to SP. Research in the Hicks lab is supported by a National Science Foundation CAREER award (MCB-1552522) awarded to LMH.

Competing interests

None declared.

Author contributions

SP designed the research; CVH, NB, PM and EWM conducted the experiment; ALS, EWM and BM analyzed the data; CVH, ALS, LMH and SP wrote the manuscript.

ORCID

Nikita Bhatnagar https://orcid.org/0000-0001-7832-1347
Chien Ha https://orcid.org/0000-0002-3119-3963
Leslie M. Hicks https://orcid.org/0000-0002-8008-3998
Parinita Majumdar https://orcid.org/0000-0002-4652-5254
Evan W. McConnell https://orcid.org/0000-0002-2295-3027
Boominathan Mohanasundaram https://orcid.org/0000-0003-1065-166X
Sona Pandey https://orcid.org/0000-0002-5570-3120
Amanda L. Smythers https://orcid.org/0000-0002-1552-6705

Data availability

The MS proteomics data have been deposited in the ProteomeXchange Consortium (www.proteomexchange.org) via the PRIDE partner repository (Vizcaíno *et al.*, 2014). Reviewers can access the data (www.ebi.ac.uk/pride/archive/login) using identifiers PXD011907 for reversible cysteine oxidation (Username: reviewer54885@ebi.ac.uk, Password: f47ZGNZB) and PXD011711 for global proteomics (Username: reviewer47263@ebi.ac.uk, Password: Jyy5bbeZ).

References

Abt MR, Pfister B, Sharma M, Eicke S, Bürgy L, Neale I, Seung D, Zeeman SC. 2020. STARCH SYNTHASE5, a noncanonical starch synthase-like protein, promotes starch granule initiation in Arabidopsis. *Plant Cell* **32**: 2543–2565.

Albert R, Acharya BR, Jeon BW, Zanudo JGT, Zhu M, Osman K, Assmann SM. 2017. A new discrete dynamic model of ABA-induced stomatal closure predicts key feedback loops. *PLoS Biology* **15**: e2003451.

Alvarez S, Hicks LM, Pandey S. 2011. ABA-dependent and -independent G-protein signaling in Arabidopsis roots revealed through an iTRAQ proteomics approach. *Journal of Proteome Research* **10**: 3107–3122.

Alvarez S, Roy Choudhury S, Hicks LM, Pandey S. 2013. Quantitative proteomics-based analysis supports a significant role of GTG proteins in regulation of ABA response in Arabidopsis roots. *Journal of Proteome Research* **12**: 1487–1501.

Alvaro CG, Thorner J. 2016. Heterotrimeric G protein-coupled receptor signaling in yeast mating pheromone response. *Journal of Biological Chemistry* **291**: 7788–7795.

Ameztoy K, Baslam M, Sánchez-López ÁM, Muñoz FJ, Bahaji A, Almagro G, García-Gómez P, Baroja-Fernández E, De Diego N, Humplík JF *et al.* 2019. Plant responses to fungal volatiles involve global posttranslational thiol redox proteome changes that affect photosynthesis. *Plant, Cell & Environment* **42**: 2627–2644.

Apel K, Hirt H. 2004. Reactive oxygen species: metabolism, oxidative stress, and signal transduction. *Annual Reviews in Plant Biology* **55**: 373–399.

Bedhomme M, Adamo M, Marchand CH, Couturier J, Rouhier N, Lemaire SD, Zaffagnini M, Trost P. 2012. Glutathionylation of cytosolic glyceraldehyde-3-phosphate dehydrogenase from the model plant *Arabidopsis thaliana* is reversed by both glutaredoxins and thioredoxins *in vitro*. *Biochemical Journal* **445**: 337–347.

Brzezowski P, Richter AS, Grimm B. 2015. Regulation and function of tetrapyrrole biosynthesis in plants and algae. *Biochimica et Biophysica Acta* **1847**: 968–985.

Chakravorty D, Gookin TE, Milner MJ, Yu Y, Assmann SM. 2015. Extra-large G proteins expand the repertoire of subunits in Arabidopsis heterotrimeric G protein signaling. *Plant Physiology* **169**: 512–529.

Chapman JM, Muhlemann JK, Gayomba SR, Muday GK. 2019. RBOH-dependent ROS synthesis and ROS scavenging by plant specialized metabolites

to modulate plant development and stress responses. *Chemical Research in Toxicology* **32**: 370–396.

Chen J-H, Jiang H-W, Hsieh E-J, Chen H-Y, Chien C-T, Hsieh H-L, Lin T-P. 2012. Drought and salt stress tolerance of an Arabidopsis glutathione-transferase U17 knockout mutant are attributed to the combined effect of glutathione and abscisic acid. *Plant Physiology* **158**: 340–351.

Chen S, Jia H, Wang X, Shi C, Wang X, Ma P, Wang J, Ren M, Li J. 2020. Hydrogen sulfide positively regulates abscisic acid signaling through persulfidation of SnRK2.6 in guard cells. *Molecular Plant* **13**: 732–744.

Choudhury FK, Rivero RM, Blumwald E, Mittler R. 2017. Reactive oxygen species, abiotic stress and stress combination. *The Plant Journal* **90**: 856–867.

Cimini S, Gualtieri C, Macovei A, Balestrazzi A, De Gara L, Locato V. 2019. Redox balance-DDR-miRNA triangle: relevance in genome stability and stress responses in plants. *Frontiers in Plant Science* **10**: 989.

Commuri PD, Keeling PL. 2001. Chain-length specificities of maize starch synthase I enzyme: studies of glucan affinity and catalytic properties. *The Plant Journal* **25**: 475–486.

Couturier J, Chibani K, Jacquot JP, Rouhier N. 2013. Cysteine-based redox regulation and signaling in plants. *Frontiers in Plant Science* **4**: 105.

Dumont S, Bykova NV, Pelletier G, Dorion S, Rivoal J. 2016. Cytosolic triosephosphate isomerase from *Arabidopsis thaliana* is reversibly modified by glutathione on cysteines 127 and 218. *Frontiers in Plant Science* **7**: 1942.

Dumont S, Rivoal J. 2019. Consequences of oxidative stress on plant glycolytic and respiratory metabolism. *Frontiers in Plant Science* **10**: 166.

Eckhardt U, Grimm B, Hörtensteiner S. 2004. Recent advances in chlorophyll biosynthesis and breakdown in higher plants. *Plant Molecular Biology* **56**: 1–14.

Fares A, Rossignol M, Peltier J-B. 2011. Proteomics investigation of endogenous S-nitrosylation in Arabidopsis. *Biochemical and Biophysical Research Communications* **416**: 331–336.

Feng Y, Forgac M. 1994. Inhibition of vacuolar H^+-ATPase by disulfide bond formation between cysteine 254 and cysteine 532 in subunit A. *Journal of Biological Chemistry* **269**: 13224–13230.

Fichman Y, Miller G, Mittler R. 2019. Whole-plant live imaging of reactive oxygen species. *Molecular Plant* **12**: 1203–1210.

Foyer CH. 2018. Reactive oxygen species, oxidative signaling and the regulation of photosynthesis. *Environmental and Experimental Botany* **154**: 134–142.

Foyer CH, Noctor G. 2003. Redox sensing and signalling associated with reactive oxygen in chloroplasts, peroxisomes and mitochondria. *Physiologia Plantarum* **119**: 355–364.

Fra A, Yoboue ED, Sitia R. 2017. Cysteines as redox molecular switches and targets of disease. *Frontiers in Molecular Neuroscience* **10**: 167.

Franks PJ, Farquhar GD. 2001. The effect of exogenous abscisic acid on stomatal development, stomatal mechanics, and leaf gas exchange in *Tradescantia virginiana*. *Plant Physiology* **125**: 935–942.

Gehan MA, Fahlgren N, Abbasi A, Berry JC, Callen ST, Chavez L, Doust AN, Feldman MJ, Gilbert KB, Hodge JG *et al.* 2017. PlantCV v.2: image analysis software for high-throughput plant phenotyping. *PeerJ* **5**: e4088.

Gleason C, Huang S, Thatcher LF, Foley RC, Anderson CR, Carroll AJ, Millar AH, Singh KB. 2011. Mitochondrial complex II has a key role in mitochondrial-derived reactive oxygen species influence on plant stress gene regulation and defense. *Proceedings of the National Academy of Sciences, USA* **108**: 10768–10773.

Gururani MA, Venkatesh J, Tran LS. 2015. Regulation of photosynthesis during abiotic stress-induced photoinhibition. *Molecular Plant* **8**: 1304–1320.

Ha CV, Leyva-Gonzalez MA, Osakabe Y, Tran UT, Nishiyama R, Watanabe Y, Tanaka M, Seki M, Yamaguchi S, Dong NV *et al.* 2014. Positive regulatory role of strigolactone in plant responses to drought and salt stress. *Proceedings of the National Academy of Sciences, USA* **111**: 851–856.

Ha J-H, Kim J-H, Kim S-G, Sim H-J, Lee G, Halitschke R, Baldwin IT, Kim J-I, Park C-M. 2018. Shoot phytochrome B modulates reactive oxygen species homeostasis in roots via abscisic acid signaling in Arabidopsis. *The Plant Journal* **94**: 790–798.

Harris CR, Millman KJ, van der Walt SJ, Gommers R, Virtanen P, Cournapeau D, Wieser E, Taylor J, Berg S, Smith NJ *et al.* 2020. Array programming with NumPy. *Nature* **585**: 357–362.

He J, Duan Y, Hua D, Fan G, Wang L, Liu Y, Chen Z, Han L, Qu L-J, Gong Z. 2012. DEXH box RNA helicase-mediated mitochondrial reactive oxygen species production in Arabidopsis mediates crosstalk between abscisic acid and auxin signaling. *Plant Cell* **24**: 1815–1833.

Hochberg YBY. 1995. Controlling the false discovery rate: a practical and powerful approach to multiple testing. *Journal of the Royal Statistical Society: Series B (Methodological)* **57**: 289–300.

Hossain MS, Dietz KJ. 2016. Tuning of redox regulatory mechanisms, reactive oxygen species and redox homeostasis under salinity stress. *Frontiers in Plant Science* **7**: 548.

Huang H, Ullah F, Zhou DX, Yi M, Zhao Y. 2019. Mechanisms of ROS regulation of plant development and stress responses. *Frontiers in Plant Science* **10**: 800.

Huang J, Taylor JP, Chen J-G, Uhrig JF, Schnell DJ, Nakagawa T, Korth KL, Jones AM. 2006. The plastid protein THYLAKOID FORMATION1 and the plasma membrane G-protein GPA1 interact in a novel sugar-signaling mechanism in Arabidopsis. *Plant Cell* **18**: 1226–1238.

Huang J, Willems P, Wei B, Tian C, Ferreira RB, Bodra N, Martínez Gache SA, Wahni K, Liu K, Vertommen D *et al.* 2019. Mining for protein S-sulfenylation in Arabidopsis uncovers redox-sensitive sites. *Proceedings of the National Academy of Sciences, USA* **116**: 21256–21261.

Huang S, Van Aken O, Schwarzländer M, Belt K, Millar AH. 2016. The roles of mitochondrial reactive oxygen species in cellular signaling and stress response in plants. *Plant Physiology* **171**: 1551–1559.

Iwai S, Ogata S, Yamada N, Onjo M, Sonoike K, Shimazaki K. 2019. Guard cell photosynthesis is crucial in abscisic acid-induced stomatal closure. *Plant Direct* **3**: e00137.

Jin Y, Chen S, Fan X, Song H, Li X, Xu J, Qian H. 2017. Diuron treatment reveals the different roles of two cyclic electron transfer pathways in photosystem II in *Arabidopsis thaliana*. *Pesticide Biochemistry and Physiology* **137**: 15–20.

Käll L, Canterbury JD, Weston J, Noble WS, MacCoss MJ. 2007. Semi-supervised learning for peptide identification from shotgun proteomics datasets. *Nature Methods* **4**: 923–925.

Kempa S, Krasensky J, Dal Santo S, Kopka J, Jonak C. 2008. A central role of abscisic acid in stress-regulated carbohydrate metabolism. *PLoS ONE* **3**: e3935.

Kuromori T, Seo M, Shinozaki K. 2018. ABA transport and plant water stress responses. *Trends in Plant Science* **23**: 513–522.

Laureano-Marín AM, Aroca A, Perez-Perez ME, Yruela I, Jurado-Flores A, Moreno I, Crespo JL, Romero LC, Gotor C. 2020. Abscisic acid-triggered persulfidation of cysteine protease ATG4 mediates regulation of autophagy by sulfide. *Plant Cell* **32**: 3902–3920.

Li Y, Liu B, Zhang J, Kong F, Zhang L, Meng H, Li W, Rochaix JD, Li D, Peng L. 2019. OHP1, OHP2, and HCF244 form a transient functional complex with the photosystem II reaction center. *Plant Physiology* **179**: 195–208.

Liang Y, Gao Y, Jones AM. 2017. Extra large G-protein interactome reveals multiple stress response function and partner-dependent XLG subcellular localization. *Frontiers in Plant Science* **8**: 1015.

Liu C, Xu Y, Long D, Cao B, Hou J, Xiang Z, Zhao A. 2017. Plant G-protein beta subunits positively regulate drought tolerance by elevating detoxification of ROS. *Biochemical and Biophysical Research Communications* **491**: 897–902.

Liu P, Zhang H, Wang H, Xia Y. 2014. Identification of redox-sensitive cysteines in the Arabidopsis proteome using OxiTRAQ, a quantitative redox proteomics method. *Proteomics* **14**: 750–762.

Liu Y, He C. 2016. Regulation of plant reactive oxygen species (ROS) in stress responses: learning from AtRBOHD. *Plant Cell Reports* **35**: 995–1007.

López-Grueso MJ, González-Ojeda R, Requejo-Aguilar R, McDonagh B, Fuentes-Almagro CA, Muntané J, Bárcena JA, Padilla CA. 2019. Thioredoxin and glutaredoxin regulate metabolism through different multiplex thiol switches. *Redox Biology* **21**: 101049.

Lu Y. 2016. Identification and roles of photosystem II assembly, stability, and repair factors in Arabidopsis. *Frontiers in Plant Science* **7**: 168.

Luo W, Pant G, Bhavnasi YK, Blanchard SG Jr, Brouwer C. 2017. Pathview Web: user friendly pathway visualization and data integration. *Nucleic Acids Research* **45**: W501–W508.

Lv B, Wei K, Hu K, Tian T, Zhang F, Yu Z, Zhang D, Su Y, Sang Y, Zhang X *et al.* 2021. MPK14-mediated auxin signaling controls lateral root development via ERF13-regulated very-long-chain fatty acid biosynthesis. *Molecular Plant* **14**: 285–297.

McConnell EW, Berg P, Westlake TJ, Wilson KM, Popescu GV, Hicks LM, Popescu SC. 2019. Proteome-wide analysis of cysteine reactivity during effector-triggered immunity. *Plant Physiology* **179**: 1248–1264.

McConnell EW, Werth EG, Hicks LM. 2018. The phosphorylated redox proteome of *Chlamydomonas reinhardtii*: revealing novel means for regulation of protein structure and function. *Redox Biology* **17**: 35–46.

Mergner J, Frejno M, List M, Papacek M, Chen X, Chaudhary A, Samaras P, Richter S, Shikata H, Messerer M *et al.* 2020. Mass-spectrometry-based draft of the Arabidopsis proteome. *Nature* **579**: 409–414.

Mittler R. 2017. ROS are good. *Trends in Plant Science* **22**: 11–19.

Nguyen HM, Sako K, Matsui A, Suzuki Y, Mostofa MG, Ha CV, Tanaka M, Tran LP, Habu Y, Seki M. 2017. Ethanol enhances high-salinity stress tolerance by detoxifying reactive oxygen species in *Arabidopsis thaliana* and rice. *Frontiers in Plant Science* **8**: 1001.

Nilson SE, Assmann SM. 2010. Heterotrimeric G proteins regulate reproductive trait plasticity in response to water availability. *New Phytologist* **185**: 734–746.

Nitta Y, Ding P, Zhang Y. 2015. Heterotrimeric G proteins in plant defense against pathogens and ABA signaling. *Environmental and Experimental Botany* **114**: 153–158.

Noctor G, Reichheld JP, Foyer CH. 2018. ROS-related redox regulation and signaling in plants. *Seminars in Cell and Developmental Biology* **80**: 3–12.

Pandey S. 2019. Heterotrimeric G-protein signaling in plants: conserved and novel mechanisms. *Annual Reviews in Plant Biology* **70**: 213–238.

Pandey S, Nelson DC, Assmann SM. 2009. Two novel GPCR-type G proteins are abscisic acid receptors in Arabidopsis. *Cell* **136**: 136–148.

Patterson JA, Tetlow IJ, Emes MJ. 2018. Bioinformatic and *in vitro* analyses of Arabidopsis starch synthase 2 reveal post-translational regulatory mechanisms. *Frontiers in Plant Science* **9**: 1338.

Postiglione AE, Muday GK. 2020. The role of ROS homeostasis in ABA-induced guard cell signaling. *Frontiers in Plant Science* **11**: 968.

Qi J, Song CP, Wang B, Zhou J, Kangasjärvi J, Zhu JK, Gong Z. 2018. Reactive oxygen species signaling and stomatal movement in plant responses to drought stress and pathogen attack. *Journal of Integrative Plant Biology* **60**: 805–826.

van der Reest J, Lilla S, Zheng L, Zanivan S, Gottlieb E. 2018. Proteome-wide analysis of cysteine oxidation reveals metabolic sensitivity to redox stress. *Nature Communications* **9**: 1581.

Roy Choudhury S, Li M, Lee V, Nandety RS, Mysore KS, Pandey S. 2020. Flexible functional interactions between G-protein subunits contribute to the specificity of plant responses. *The Plant Journal* **102**: 207–221.

Sanchez-Fernandez G, Cabezudo S, Garcia-Hoz C, Beninca C, Aragay AM, Mayor F Jr, Ribas C. 2014. Galphaq signalling: the new and the old. *Cellular Signalling* **26**: 833–848.

Santelia D, Trost P, Sparla F. 2015. New insights into redox control of starch degradation. *Current Opinion in Plant Biology* **25**: 1–9.

Seidel T, Scholl S, Krebs M, Rienmüller F, Marten I, Hedrich R, Hanitzsch M, Janetzki P, Dietz K-J, Schumacher K. 2012. Regulation of the V-type ATPase by redox modulation. *Biochemical Journal* **448**: 243–251.

Shen J, Zhang J, Zhou M, Zhou H, Cui B, Gotor C, Romero LC, Fu L, Yang J, Foyer CH *et al.* 2020. Persulfidation-based modification of cysteine desulfhydrase and the NADPH oxidase RBOHD controls guard cell abscisic acid signaling. *Plant Cell* **32**: 1000–1017.

Slade WO, Werth EG, McConnell EW, Alvarez S, Hicks LM. 2015. Quantifying reversible oxidation of protein thiols in photosynthetic organisms. *The Journal of the American Society for Mass Spectrometry* **26**: 631–640.

Smythers AL, Hicks LM. 2021. Mapping the plant proteome: tools for surveying coordinating pathways. *Emerging Topics in Life Sciences* **5**: 203–220.

Smythers AL, McConnell EW, Lewis HC, Mubarek SN, Hicks LM. 2020. Photosynthetic metabolism and nitrogen reshuffling are regulated by reversible cysteine thiol oxidation following nitrogen deprivation in *Chlamydomonas*. *Plants* **9**: 784.

Song Y, Miao Y, Song C-P. 2014. Behind the scenes: the roles of reactive oxygen species in guard cells. *New Phytologist* **201**: 1121–1140.

Suzuki N, Miller G, Salazar C, Mondal HA, Shulaev E, Cortes DF, Shuman JL, Luo X, Shah J, Schlauch K. 2013. Temporal-spatial interaction between reactive oxygen species and abscisic acid regulates rapid systemic acclimation in plants. *Plant Cell* **25**: 3553–3569.

Takahashi F, Kuromori T, Sato H, Shinozaki K. 2018. Regulatory gene networks in drought stress responses and resistance in plants. *Advances in Experimental Medicine and Biology* **1081**: 189–214.

Tavakoli N, Kluge C, Golldack D, Mimura T, Dietz KJ. 2001. Reversible redox control of plant vacuolar H^+–ATPase activity is related to disulfide bridge formation in subunit E as well as subunit A. *The Plant Journal* **28**: 51–59.

Thalmann M, Pazmino D, Seung D, Horrer D, Nigro A, Meier T, Kölling K, Pfeifhofer HW, Zeeman SC, Santelia D. 2016. Regulation of leaf starch degradation by abscisic acid is important for osmotic stress tolerance in plants. *Plant Cell* **28**: 1860–1878.

Ton J, Flors V, Mauch-Mani B. 2009. The multifaceted role of ABA in disease resistance. *Trends in Plant Science* **14**: 310–317.

Torres MA, Morales J, Sanchez-Rodriguez C, Molina A, Dangl JL. 2013. Functional interplay between Arabidopsis NADPH oxidases and heterotrimeric G protein. *Molecular Plant–Microbe Interactions* **26**: 686–694.

Ullah H, Chen JG, Temple B, Boyes DC, Alonso JM, Davis KR, Ecker JR, Jones AM. 2003. The beta-subunit of the Arabidopsis G protein negatively regulates auxin-induced cell division and affects multiple developmental processes. *Plant Cell* **15**: 393–409.

Urano D, Miura K, Wu Q, Iwasaki Y, Jackson D, Jones AM. 2016. Plant morphology of heterotrimeric G protein mutants. *Plant and Cell Physiology* **57**: 437–445.

Vizcaíno JA, Deutsch EW, Wang R, Csordas A, Reisinger F, Ríos D, Dianes JA, Sun Z, Farrah T, Bandeira N *et al.* 2014. ProteomeXchange provides globally coordinated proteomics data submission and dissemination. *Nature Biotechnology* **32**: 223–226.

Watkins JM, Chapman JM, Muday GK. 2017. Abscisic acid-induced reactive oxygen species are modulated by flavonols to control stomata aperture. *Plant Physiology* **175**: 1807–1825.

Wu J, Zhang N, Liu Z, Liu S, Liu C, Lin J, Yang H, Li S, Yukawa Y. 2020. The AtGSTU7 gene influences glutathione-dependent seed germination under ABA and osmotic stress in Arabidopsis. *Biochemical and Biophysical Research Communications* **528**: 538–544.

Xu DB, Chen M, Ma YN, Xu ZS, Li LC, Chen YF, Ma YZ. 2015. A G-protein β subunit, AGB1, negatively regulates the ABA response and drought tolerance by down-regulating AtMPK6-related pathway in Arabidopsis. *PLoS ONE* **10**: e0116385.

Xu P, Lian H, Xu F, Zhang T, Wang S, Wang W, Du S, Huang J, Yang HQ. 2019. Phytochrome B and AGB1 coordinately regulate photomorphogenesis by antagonistically modulating PIF3 stability in Arabidopsis. *Molecular Plant* **12**: 229–247.

Ying J, Clavreul N, Sethuraman M, Adachi T, Cohen RA. 2007. Thiol oxidation in signaling and response to stress: detection and quantification of physiological and pathophysiological thiol modifications. *Free Radical Biology & Medicine* **43**: 1099–1108.

Yoshida T, Obata T, Feil R, Lunn JE, Fujita Y, Yamaguchi-Shinozaki K, Fernie AR. 2019. The role of abscisic acid signaling in maintaining the metabolic balance required for Arabidopsis growth under nonstress conditions. *Plant Cell* **31**: 84–105.

Yu Y, Assmann SM. 2015. The heterotrimeric G-protein beta subunit, AGB1, plays multiple roles in the Arabidopsis salinity response. *Plant, Cell & Environment* **38**: 2143–2156.

Yuan GL, Li HJ, Yang WC. 2017. The integration of Gbeta and MAPK signaling cascade in zygote development. *Scientific Reports* **7**: 8732.

Zandalinas SI, Mittler R, Balfagon D, Arbona V, Gomez-Cadenas A. 2018. Plant adaptations to the combination of drought and high temperatures. *Physiologia Plantarum* **162**: 2–12.

Zhou XF, Jin YH, Yoo CY, Lin X-L, Kim W-Y, Yun D-J, Bressan RA, Hasegawa PM, Jin JB. 2013. CYCLIN H;1 regulates drought stress responses and blue light-induced stomatal opening by inhibiting reactive oxygen species accumulation in Arabidopsis. *Plant Physiology* **162**: 1030–1041.

Zhu M, Zhu N, Song WY, Harmon AC, Assmann SM, Chen S. 2014. Thiol-based redox proteins in abscisic acid and methyl jasmonate signaling in *Brassica napus* guard cells. *The Plant Journal* **78**: 491–515.

Supporting Information

Additional Supporting Information may be found online in the Supporting Information section at the end of the article.

Fig. S1 Abscisic acid- and G-protein-dependent oxidation changes in proteins related to plant–pathogen interaction.

Fig. S2 Abscisic acid- and G-protein-dependent oxidation changes in proteins related to glutathione metabolism.

Fig. S3 Abscisic acid- and G-protein-dependent oxidation changes in proteins related to peroxisome metabolism.

Fig. S4 Abscisic acid- and G-protein-dependent oxidation changes in proteins related to fatty acid degradation.

Fig. S5 Abscisic acid- and G-protein-dependent oxidation changes in proteins involved in photosynthesis and antenna complex.

Fig. S6 Abscisic acid- and G-protein-dependent oxidation changes in proteins involved in glycolysis and gluconeogenesis.

Fig. S7 Abscisic acid- and G-protein-dependent oxidation changes in proteins involved pentose phosphate pathway.

Fig. S8 Abscisic acid- and G-protein-dependent oxidation changes in proteins involved oxidative phosphorylation.

Fig. S9 Physiological characterization of *mapk14* mutants.

Table S1 Global proteomic analysis of all quantified proteins.

Table S2 PANTHER overrepresentation test of all proteins quantified in this study.

Table S3 Redox proteomic analysis of all quantified identifiers.

Table S4 PANTHER overrepresentation test of all redox identifiers quantified in this study.

Table S5 Redox proteomic analysis of all identifiers related to specific pathways that meet the threshold for significance in at least one paired comparison.

Please note: Wiley Blackwell are not responsible for the content or functionality of any Supporting Information supplied by the authors. Any queries (other than missing material) should be directed to the *New Phytologist* Central Office.